Astron. Astrophys. 330, 90–96 (1998)

ASTRONOMY AND ASTROPHYSICS

Limits on magnetic fields and relativistic electrons in the Coma cluster from multifrequency observations

Torsten A. Enßlin and Peter L. Biermann

Max-Planck-Institut für Radioastronomie, Auf dem Hügel 69, D-53121 Bonn, Germany
(ensslin@mpifr-bonn.mpg.de, plbiermann@mpifr-bonn.mpg.de)

Received 22 May 1997 / Accepted 24 September 1997

Abstract. Relativistic electrons, seen in the large diffuse radio halo of the Coma cluster of galaxies, should scatter background photons to higher energies. We calculate the inverse Compton contributions from the microwave background, from the local radiation field of elliptical galaxies and from the thermal X-ray emission of the intra cluster medium to the different observed energy bands, and draw restrictions to the shape of the spectrum of the relativistic electron population. The expected electron spectra in different halo formation models are discussed, and signatures for a future distinction of these models are presented, tracing the injection processes and the influence of optical thickness of the radio halo for very low frequency emission due to synchrotron self absorption. Some of the upper limits on the electron spectrum translate into lower limits of the halo magnetic fields, since the observed synchrotron radiation is known. Despite uncertainties in the extrapolation of the radio spectrum to lower frequencies a lower limit to the central field strength of $B_\mathrm{o} > 0.3\,\mu$G seems to be sure. This is comparable to the value resulting from minimal energy arguments. If $B_\mathrm{o} \leq 1.2\,\mu$G, the recently reported extreme ultraviolet excess of Coma (Lieu et al. 1996) could result from inverse Compton scattered microwave photons. Formulae for transrelativistic Thomson scattering are given in the Appendix.

Key words: magnetic fields – galaxies: clusters: individual: Coma – galaxies: intergalactic medium – radiation mechanism: non-thermal – radio continuum: general

1. Introduction

An estimate of a lower limit on the magnetic field strength in the Coma halo region by Rephaeli et al. (1994) is $B > 0.1\,\mu$G, using the radio spectra of the halo and an upper limit to inverse Compton (IC) photons in the hard X-ray region measured by the OSSE experiment. The limit on the field strength derived from the upper limit to the gamma-ray flux above 100 MeV by EGRET resulting from relativistic bremsstrahlung is $B > 0.4\,\mu$G (Sreekumar et al. 1996), if the radio spectrum can be extrapolated to lower frequencies. The field strength, derived by Kim et al. (1986), resulting from minimal energy arguments is $B \approx 0.6\,\mu\mathrm{G}\,(1 + k_\mathrm{p})^{2/7}\,h_{50}^{2/7}$, where k_p is the proton to electron energy ratio. Measurements of Faraday rotation of polarized radiation seen through the Coma cluster medium, combined with gas profiles, derived from X-ray observations of the hot intra cluster medium (ICM), give magnetic fields of $1.7\,\mu\mathrm{G}\,(l_\mathrm{frs}/10\,\mathrm{kpc})^{-1/2}\,h_{50}^{1/2}$ (Kim et al. 1990) and $6.0\,\mu\mathrm{G}\,(l_\mathrm{frs}/1\,\mathrm{kpc})^{-1/2} h_{50}^{1/2}$ (Feretti et al. 1995). l_frs denotes the field reversal scale of the magnetic field and can in principle be measured by depolarization observations. In both measurements the resolution of l_frs was limited by the resolution of the telescope, and therefore higher field values could result from a smaller field reversal scale. Strong magnetic fields on the order of a few tens of μG are expected from the injection of radio plasma from radio galaxies into the ICM (Enßlin et al. 1997). Although field limits derived by IC flux limits are lower than the rotation measurements, they have the advantage of being less independent of the model. Quantities in this article are scaled to a Hubble constant of $H_\mathrm{o} = 50\,\mathrm{km\,s^{-1}\,Mpc^{-1}}\,h_{50}$, where h_{50} indicates their scaling.

2. Multifrequency observations

2.1. Radio

The radio flux spectrum of the diffuse radio halo Coma C

$$F_\nu = (8.3 \pm 1.5) \cdot 10^{-12} \left(\frac{\nu}{\mathrm{Hz}}\right)^{-1.34\pm0.06} \frac{\mathrm{erg}}{\mathrm{cm^2\,s\,Hz}} \qquad (1)$$

(Kim et. al 1990) results from a relativistic electron population, which we assume to be

$$N_\mathrm{e}(r, \beta_\mathrm{e}\gamma_\mathrm{e})\,d(\beta_\mathrm{e}\gamma_\mathrm{e}) = C_\mathrm{e}(r)\,(\beta_\mathrm{e}\gamma_\mathrm{e})^{-\alpha}\,d(\beta_\mathrm{e}\gamma_\mathrm{e}) \qquad (2)$$

with a spectral index $\alpha = 3.68 \pm 0.12$. $P_\mathrm{e} = \beta_\mathrm{e}\gamma_\mathrm{e}\,m_\mathrm{e}\,c$ is the electron momentum, and β_e should not be confused with the cluster shape parameter β. The synchrotron flux of a power law electron distribution in an isotropic distribution of magnetic

fields within the halo volume (Eq. (6.36) in Rybicki & Lightman 1979), averaged over an isotropic distribution of electron pitch angles, is

$$F_\nu = \frac{\sqrt{3} e^3 B_\mathrm{o} C_\mathrm{eo}}{m_\mathrm{e} c^2} f_\mathrm{sync}(\alpha) \left(\frac{\nu}{\nu_\mathrm{o}}\right)^{-\frac{\alpha-1}{2}} \frac{\tilde{V}_\mathrm{sync}}{4\pi D^2} \quad (3)$$

$$f_\mathrm{sync}(\alpha) = \frac{\sqrt{\pi}\,\Gamma(\frac{\alpha}{4}+\frac{19}{12})\,\Gamma(\frac{\alpha}{4}-\frac{1}{12})\,\Gamma(\frac{\alpha+5}{4})}{2\,(\alpha+1)\,\Gamma(\frac{\alpha+7}{4})} \; . \quad (4)$$

B_o, C_eo are taken at the cluster center, $D = 139\,\mathrm{Mpc}\,h_{50}^{-1}$ is the distance to Coma, Γ is the gamma function, and $\nu_\mathrm{o} = 3eB_\mathrm{o}/(2\pi m_\mathrm{e} c)$. We assume that magnetic field energy density and relativistic electron density scale radially with the same β-profile as the background gas does, $\sim (1+(r/r_\mathrm{c})^2)^{-3\beta/2}$ with $\beta = 0.75$ and $r_\mathrm{c} = 400$ kpc (Briel et al. 1992). This is reasonable since every possible source of magnetic fields such as injection by radio galaxies, compression of primordial fields frozen into the plasma, and amplification of fields by turbulent gas motion should result in a rough scaling of the magnetic energy density with the thermal energy density. Similar arguments hold for the supply of the relativistic electron population. But the best support of this assumption is given by Fig. 3 of Deiss et al. (1997), which compares the radial X-ray profile with the radio profile of the cluster, and shows that the latter is steeper. The X-ray emission scales with the gas density as $\sim n_\mathrm{e}^2(r)$, and the radio emission as $\sim C_\mathrm{e}(r)\,B^{(\alpha+1)/2}(r) \sim n_\mathrm{e}^{2.17}(r)$, and is therefore a little bit steeper, if we use the scaling assumed above ($B^2(r) \sim C_\mathrm{e}(r) \sim n_\mathrm{e}(r)$). The resulting projected emission profile is similar to that measured by Deiss et al. (1997). The emission profile itself is shown in Fig. 2.

The emission weighted volume within the halo radius, which is at least $R = 1.2\,\mathrm{Mpc}\,h_{50}^{-1}$ (Deiss et al. 1997), is given by

$$\tilde{V}_\mathrm{sync} = 2\,\pi\,\phi_B\,r_\mathrm{c}^3\,\mathscr{B}_{\frac{R^2}{R^2+r_\mathrm{c}^2}}\left(\tfrac{3}{2},\tfrac{3}{2}\left(\tfrac{\alpha+5}{4}\beta-1\right)\right) \; , \quad (5)$$

where $\mathscr{B}_x(a,b)$ denotes the unnormalized incomplete beta function (Eq. (6.6.1) Abramowitz & Stegun 1965), and should not be confused with the symbols for the field strength $B(r)$ and B_o. ϕ_B is the filling factor of the magnetic field in the volume occupied by the relativistic electrons, which we expect to be close to unity. Comparing Eq. 1 and Eq. 3 gives

$$C_\mathrm{eo} = 3.28\cdot 10^{-3}\,\mathrm{cm}^{-3}\,h_{50}\,\phi_B^{-1}\left(\frac{B_\mathrm{o}}{\mu\mathrm{G}}\right)^{-2.34} \; . \quad (6)$$

2.2. Infrared

Wise et al. (1993) searched extensively for diffuse far-infrared emission from clusters, and detected Coma marginally at 60 μm, but not at 100 μm. Their estimate of the excess fluxes above the background within 30 arcmin of the cluster center are 5 ± 4 and 1 ± 10 mJy arcmin^{-2}. (1 arcmin = 39 h_{50}^{-1} kpc). We use two sigma upper limits in the following, namely 13 and 21 mJy arcmin^{-2}.

2.3. Extreme ultraviolet

Recently, Lieu et al. (1996) have reported the detection of extended, extreme ultraviolet emission from the cluster center with the Extreme Ultraviolet Explorer (EUVE). They interpret this as evidence for relatively cold gas components with temperatures of $kT = 0.07$ and 0.4 keV. But Dixon et al. (1996) tried to detect resonance line emission with the Hopkins Ultraviolet Telescope (HUT), which would be expected in this case. Their nondetection does not reject the thermal gas model completely, but gives additional constraint on the properties of the cooler ICM components. The EUV emission might also arise from inverse Compton scattering of microwave or starlight photons, giving then direct informations about the relativistic electron population. On the other hand, if the real nature of this emission can be proven to be different from IC, then we can interpret their flux as an upper limit to any possible IC contribution, and therefore giving an upper limit to the electrons. If the detailed physics of such an emission process can be understood, this limit could be improved.

Their EUVE observation covered a field with a radius of 30 arcmin centered on the X-ray center of Coma, and they detected emission within the central 15 arcmin. The count rate in the passband of 65 to 245 eV was 36 % above the expected count rate from the emission of the thermal gas with kT = 8.2 keV. We estimate the latter flux in this band to be $8.1\cdot 10^{-2}\,\mathrm{cm}^{-2}\,\mathrm{s}^{-1}$, using their emission measure, which is in good agreement with that expected from the β-model of the gas with a central gas density of $3\cdot 10^{-3}\,\mathrm{cm}^{-3}\,h_{50}^{-1/2}$, and using the Bremsstrahlung formulae given in Novikov & Thorne (1972). This translates to an excess flux of $2.9\cdot 10^{-2}\,\mathrm{cm}^{-2}\,\mathrm{s}^{-1}$, which we use as an upper limit to the IC flux in the 65 to 245 eV passband in the following.

2.4. High energy X-rays and gamma-rays

Rephaeli et al. (1994) measured the high energy X-ray (HEX) flux from Coma with OSSE to be lower than $6\cdot 10^{-6}\mathrm{cm}^{-2}\,\mathrm{s}^{-1}\,\mathrm{keV}^{-1}$ within the 40-80 keV band. The EGRET flux limit on gamma rays from Coma is $F_\gamma(E_\gamma > 100\,\mathrm{MeV}) < 4\cdot 10^{-8}\mathrm{cm}^{-2}\,\mathrm{s}^{-1}$ (Sreekumar et al. 1996).

3. Inverse Compton emission

3.1. Coma's electron population

Only two regions of the electron spectrum are visible: the X-ray emitting thermal bulk with a temperature of 8.2 keV and relativistic electrons around 1 GeV visible in the radio. Outside of these regions information can be obtained from the detection or nondetection of IC flux resulting from electrons and background photon fields, mainly the microwave background (MWB) and the starlight of the cluster members. The radio photons of the halo do not contribute significantly to the IC flux: The energy density of the radio emission is of the order of $L_\mathrm{radio}/(4\pi\,c\,r_\mathrm{c}^2) \approx 10^{-7}\,\mathrm{eV\,cm}^{-3}$ and therefore 6 orders of magnitude lower than that of the MWB. The limits resulting

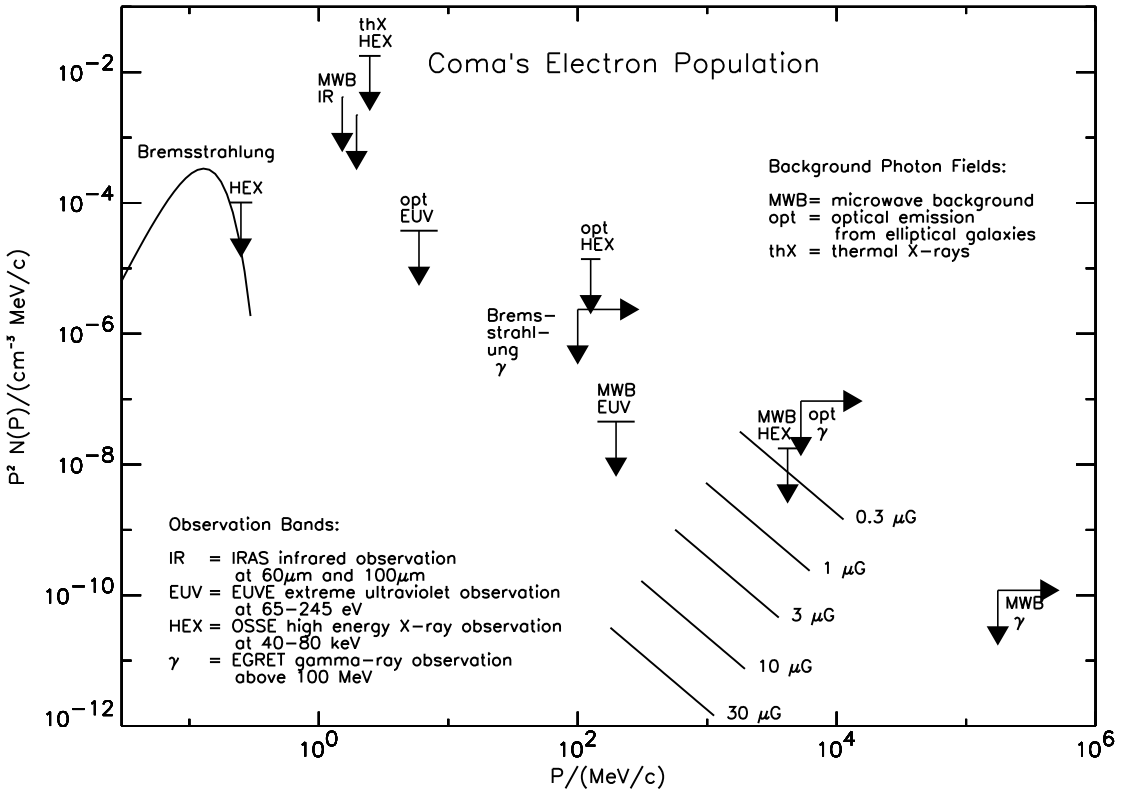

Fig. 1. The central electron population of Coma. The line labeled with 'Bremsstrahlung' shows the thermal population. Also limits from bremsstrahlung in the OSSE and EGRET bands are shown. The other lines result from radio observations and are labeled with the corresponding central field strength. Limits from inverse Compton scattering are labeled with the relevant photon population and the resulting energy range. All limits are two sigma limits except the EUV limits, which result from a detected flux, and might be read as data points, if the EUV emission results from inverse Compton scattering instead from a cool ICM component. A horizontal line in this diagram corresponds to a power law $N_{\rm e}(P_{\rm e}) \sim P_{\rm e}^{-2}$.

from the different combination of photon fields and observation bands are given in Tab. 1 and plotted in Fig. 1 above the typical electron momenta necessary to scatter the peaks of the blackbody spectra into the observation bands from the relation $<\varepsilon>=\frac{4}{3}\,\gamma_{\rm e}^2\,2.70\,kT$ (Blumenthal & Gould 1970). For the calculations, which are explained below, the spectral index of the radio electrons is used.

3.2. Microwave background

The expected IC flux from the MWB is (derived from Eq. (7.31) in Rybicki & Lightman (1979) for Thomson scattering)

$$F_\gamma(>E_\gamma) = \frac{\tilde{V}_{\rm IC}}{4\pi D^2}\,\frac{8\pi^2 r_{\rm e}^2}{h^3c^2}\,(kT)^3\,f_{\rm IC}(\alpha)\,C_{\rm eo}\left(\frac{E_\gamma}{kT}\right)^{-\frac{\alpha-1}{2}} \quad (7)$$

$$f_{\rm IC}(\alpha) = \frac{2^{\alpha+4}(\alpha^2+4\alpha+11)}{(\alpha+3)^2(\alpha+5)(\alpha^2-1)}\,\Gamma\left(\tfrac{\alpha+5}{2}\right)\zeta\left(\tfrac{\alpha+5}{2}\right) \quad (8)$$

$$\tilde{V}_{\rm IC} = 2\,\pi\,r_{\rm c}^3\cdot\mathscr{B}_{\frac{R_{\rm o}^2}{R_{\rm o}^2+r_{\rm c}^2}}\left(\tfrac{3}{2},\tfrac{3}{2}\,(\beta-1)\right)\,, \quad (9)$$

where ζ denotes the Riemann zeta function, and $R_{\rm o}$ the radius covered by the observation. The electrons seen in the radio scatter microwave photons into the hard X-ray band. Thus, with the help of Eq. 6 we can use their limit in order to get a lower limit on the central field strength of $B_{\rm o} > 0.2\,\mu{\rm G}\,\phi_B^{-0.43}h_{50}^0$, which is independent of the Hubble constant. Assuming a uniform magnetic field strength over the whole cluster volume by setting $\beta = 0$, gives only $B_{\rm o} > 0.1\,\mu{\rm G}\,\phi_B^{-0.43}h_{50}^0$, in agreement with the value of Rephaeli et al. (1994). But this is an unrealistic configuration, as explained in Sect. 2.1.

Since none of the halo formation theories discussed in Sect. 4 predicts any break in the electron spectrum between 100 MeV/c and GeV/c, it is reasonable to extrapolate the spectrum and use the limit given by the EUV flux to predict a field strength stronger than

$$B_{\rm o} > 1.2\,\mu{\rm G}\left(\frac{\phi_B\;F_{EUV,IC-limit}}{0.16/({\rm cm^2\,s\,keV})}\right)^{-0.43}\,. \quad (10)$$

If the EUV IC contribution can be further constrained, a higher field strength would follow. A break by 0.5 in the radio spectral index, placed at the lowest observed frequency of 30.9 MHz (Henning 1989) still gives a limit $B_{\rm o} > 0.3\,\mu{\rm G}\,\phi_B^{-0.54}$.

Table 1. The IC limits on the normalization constant $C_{\rm eo}$ of the power law electron distribution (Eq. 2) resulting from the different combinations of background photon fields and observation bands, and the typical electron momenta necessary for this scattering.

			$\rm IR_{60\mu m}$	$\rm IR_{100\mu m}$	$\rm EUV_{65-245eV}$	$\rm HEX_{40-80keV}$	$\rm gamma_{>100MeV}$
MWB	$P_{\rm e}$	$[MeV/c]$	1.5	2.0	$142-275$	$(3.5-5.0)\cdot 10^3$	$> 1.8\cdot 10^5$
	$C_{\rm eo}$	$[\rm cm^{-3}\,h_{50}]$	$5.1\cdot 10^{-2}$	$4.1\cdot 10^{-2}$	$2.1\cdot 10^{-3}$	0.13	0.47
optical photons	$P_{\rm e}$	$[MeV/c]$			$4.3-8.3$	$106-150$	$> 5.3\cdot 10^3$
	$C_{\rm eo}$	$[\rm cm^{-3}\,h_{50}]$			$4.4\cdot 10^{-3}$	0.28	1.0
thermal X-rays	$P_{\rm e}$	$[MeV/c]$				$2.0-3.0$	Klein-Nishina
	$C_{\rm eo}$	$[\rm cm^{-3}\,h_{50}]$				0.49	suppressed

3.3. Optical photons

The luminosity of elliptical galaxies within the central 700 arcmin^2 is given by an integration of the R-band luminosity function of Secker & Harris (1996) plus the luminosities of NGC 4874 and NGC 4889 (Strom & Strom 1978), which are not included in this luminosity function. We assume that this radiation has a blackbody spectrum with a typical temperature of 3000 K, and therefore use a bolometric correction of $m_{\rm R} - m_{\rm bol} = 1.3$ (Webbink & Jeffers 1969). The radial emission profile is that of the galaxy distribution. $\varepsilon(r') \sim (1+(r'/r_{\rm G})^2)^{-\alpha_{\rm G}}$, with $\alpha_{\rm G} = 0.8$ and $r_{\rm G} = 160\,{\rm kpc}\,h_{50}^{-1}$ (Girardi et al. 1995), which we use up to a radius of $R_{\rm G} = 5\,{\rm Mpc}\,h_{50}^{-1}$. We estimate a central bolometric emissivity of $\varepsilon_{\rm o} = 1.0\cdot 10^{13}\,L_\odot\,{\rm Mpc}^{-3}\,h_{50}$. In order to get the photon density field at a position $\boldsymbol{r}$, this has to be folded with the radiation field of a source at $\boldsymbol{r}'$: $n_\gamma(\boldsymbol{r},\boldsymbol{r}') = \varepsilon(r')/(4\pi c|\boldsymbol{r}-\boldsymbol{r}'|^2)$. Integrating over all possible angles between $\boldsymbol{r}$ and $\boldsymbol{r}'$ gives the photon density

$$n_\gamma(r) = \frac{1}{2\,c\,r}\int_o^{R_{\rm G}} dr'\,r'\,\varepsilon(r')\,\ln\frac{r+r'}{|r-r'|}\ . \qquad (11)$$

Normalizing this by dividing with the photon density of a blackbody cavity, and integrating it together with the normalized β-profile of the relativistic electrons numerically over the volume gives the effective volume $\tilde{V}_{\rm IC}$, which replaces Eq. 9. The scattering of optical photons into the EGRET band needs electrons, visible in the radio. Thus a limit of $B_{\rm o} > 0.1\,\mu{\rm G}\,\phi_B^{-0.43}$ can be set. The assumed temperature of the radiation mainly enters this calculation by the bolometric correction. The anisotropy of the optical photon field at a given position does not change the resulting IC flux of the cluster, since the integration over shells of constant radius averages the different contributions.

3.4. Thermal and nonthermal X-ray photons

The radial density profile of X-ray photons is also described by Eq. 11, with an emissivity profile $\varepsilon(r') \sim n_{\rm e}^2(r') \sim (1 + (r'/r_{\rm c})^2)^{-3\beta}$. We calculated the spectrum of the Bremsstrahlung using the Gaunt factor given in Novikov & Thorne (1972), a central gas density of $n_{\rm e,o} = 3\cdot 10^{-3}\,{\rm cm}^{-3}\,{\rm h}_{50}^{1/2}$, and a gas temperature of $kT = 8.2$ keV (Briel et al. 1992). The IC scattering of these photons had to be calculated numerically. The contribution to the EGRET band is negligible, due to the reduction of the IC cross section in the Klein-Nishina regime. The calculation of the scattering into the OSSE band was done using the exact probability distribution of frequency shifts of Thomson scattering, valid from non- to ultrarelativistic electron momenta, which is derived in the Appendix.

The limit resulting from the expected bremsstrahlung in the OSSE band of a suprathermal electron distribution is $C_{\rm eo} < 6\cdot 10^{-5}\,{\rm cm}^{-3}\,h_{50}^{1/2}$. Bremsstrahlung of relativistic electrons was calculated with the formulae in Blumenthal & Gould (1970). The EGRET limit translates into $C_{\rm eo} < 3.3\cdot 10^{-2}\,{\rm cm}^{-3}\,h_{50}^{1/2}$. These limits are also shown in Fig 1.

4. Radio halo formation

The slope of the electron spectrum is determined by the acceleration, cooling and injection processes. Three sources for the energetic electrons have been discussed in the literature:

- The *primary electron model* (Jaffe 1977, Rephaeli 1979), in which the electrons diffuse out of radio galaxies and form the radio halo. Their spectrum should be a straight power law. A steepening of the spectral index appears at a break frequency, if there is some momentum dependent escape from the halo region.
- In the *in-situ acceleration model* (Jaffe 1977, Roland et al. 1981, Schlickeiser et al. 1987, Burns et al. 1994, Deiss et al. 1997) the electrons are accelerated within the ICM by plasma waves or shocks. Burns et al. (1994) report evidence for a recent merger event of Coma ~ 2 Gyr ago, which was strong enough to power the radio halo. An exponential cutoff in the spectrum should occur at the momentum, where the cooling time scale gets comparable to the acceleration time scale.
- The *secondary electron model* (Dennison 1980) assumes the relativistic electrons, but also positrons, to result from pion decay after hadronic interaction of a relativistic proton population with the background gas. Since the protons should result from radio galaxies (Enßlin et al. 1997) and supernova remnants in starburst galaxies (Völk et al. 1996), which are able to accelerate to high energies, no cutoff in the electron spectrum is expected. But the injection spectrum peaks at 35 MeV/c (due to the kinematics of the decay $\pi^\pm \rightarrow \nu_\mu\mu^\pm, \mu^\pm \rightarrow \nu_\mu\nu_e e^\pm$), and therefore the equilibrium spectrum should flatten to a spectral index $\alpha = 2$ (due to synchrotron and IC cooling) below the main injection energy range.

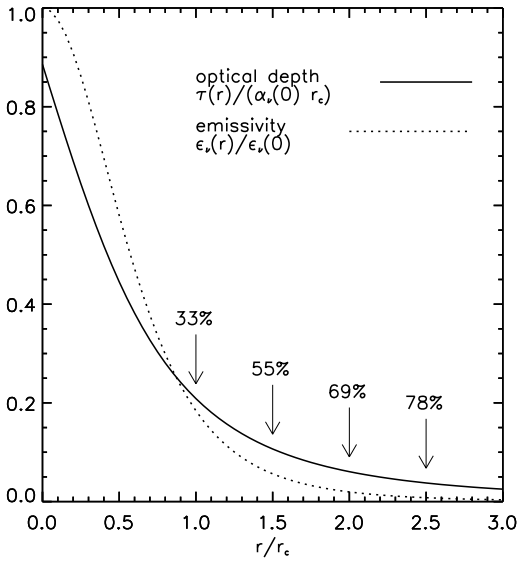

Fig. 2. Normalized optical depth $\tau(r)$ for synchrotron self absorption (solid) and synchrotron emissivity $\varepsilon_\nu(r)$ (dotted) as a function of radius. The numbers indicate the percentage of total emission produced within the indicated radius. A radial unlimited emission region was assumed for simplicity.

Schlickeiser et al. (1987) report a high frequency cutoff in the radio spectrum of the halo at 2.7 GHz, which would indicate a cutoff in the electron distribution, and therefore supports the *in-situ acceleration model*. But Deiss et al. (1997) claim that their much higher measured flux at 1.4 GHz is not consistent with the value of Schlickeiser et al. (1987). Deiss et al. (1997) suspect that the value of the flux given by these authors is much too low, which implies that the claimed strong steepening of the spectrum above 1.4 GHz is not real. In the literature (e.g. Schlickeiser et al. (1987) or Deiss et al. (1997)) citations of an upper flux limit at 5 GHz appear frequently, measured by Waldthausen (1980). But his observation was restricted to the central region of the Coma cluster, and therefore no proper background determination was possible. In order to clarify the question about the existence of a cutoff in the electron distribution, which is important for models of halo formation, new high frequency observations of the diffuse radio halo are necessary.

The low energy spectral break expected in the *secondary electron model* cannot be used easily for a distinction between the models, since we expect a sharp step in the spectrum in the same energy range, which could make it difficult to detect the appearance of the break. This step is caused by a sharp change in the cooling time scale as a function of energy, due to the transition from optical thin synchrotron emission at higher energies to optically thick emission below the step energy. In the optical thick regime, the radio power emitted by the electrons is reabsorbed, and therefore synchrotron cooling is suppressed. The synchrotron self absorption coefficient (Eq. (6.53) in Rybicki & Lightman 1979) averaged over an isotropic distribution of electron pitch angles is

$$\alpha_\nu = \frac{\sqrt{3}\, e^3\, B\, C_\mathrm{e}}{8\pi m_\mathrm{e}\, \nu_\mathrm{o}^2}\, f_\mathrm{a}(\alpha) \left(\frac{\nu}{\nu_\mathrm{o}}\right)^{-\frac{\alpha+4}{2}} \tag{12}$$

$$f_\mathrm{a}(\alpha) = \frac{\sqrt{\pi}\,\Gamma(\frac{\alpha+6}{4})\,\Gamma(\frac{3\alpha+2}{12})\,\Gamma(\frac{3\alpha+22}{12})}{2\,\Gamma(\frac{\alpha+8}{4})}\ , \tag{13}$$

and can be evaluated at the cluster center using Eq. 6:

$$\alpha_\nu(0) = \frac{342}{r_\mathrm{c}} \left(\frac{\nu}{0.1\,\mathrm{MHz}}\right)^{-3.84} \left(\frac{B_\mathrm{o}}{\mu\mathrm{G}}\right)^{\frac{1}{2}} \tag{14}$$

$$= \frac{3.9}{r_\mathrm{c}} \left(\frac{P_\mathrm{e}}{0.1\,\mathrm{GeV/c}}\right)^{-7.68} \left(\frac{B_\mathrm{o}}{\mu\mathrm{G}}\right)^{-3.34}\ , \tag{15}$$

where the frequency was translated to electron momentum using the monochromatic approximation $\nu = (\beta_\mathrm{e}\gamma_\mathrm{e})^2\,\nu_o$. The optical depth $\tau(r)$ at a radius r is given by an integral from that radius to infinity over the radial profile of the absorption coefficient

$$\alpha_\nu(r) \sim C_\mathrm{e}(r)\, B(r)^{\frac{\alpha+2}{2}} \sim \left[1+(r/r_\mathrm{c})^2\right]^{-\frac{3(\alpha+6)}{8}\beta}\ , \tag{16}$$

and is plotted in Fig. 2. Most of the total power at a given frequency is emitted within 2 core radii, and would result from a region with optical depth bigger than one if the central absorption coefficient is $\alpha_\nu(0) > 1/(0.05\, r_\mathrm{c})$. This happens for $\nu < \tilde{\nu} = 21\,\mathrm{kHz}\ (B_\mathrm{o}/\mu\mathrm{G})^{0.13}$ corresponding to $P_\mathrm{e} < \tilde{P}_\mathrm{e} = 81\,\mathrm{MeV/c}\ (B_\mathrm{o}/\mu\mathrm{G})^{-0.43}$. This sudden change in the radio spectrum can hardly be detected, but should make a signature in a halo electron population, which was injected at higher energies and cools by IC and synchrotron losses, as it is the case for the *primary* and *secondary electron model*. The time independent solution of the continuity equation for these electrons in momentum space is

$$N_\mathrm{e}(P_\mathrm{e}) = \frac{1}{b(P_\mathrm{e})} \int_{P_\mathrm{e}}^{\infty} dp\, q_\mathrm{e}(p)\ , \tag{17}$$

where $q_\mathrm{e}(p)$ is the injection spectrum and

$$b(P_\mathrm{e}) = \frac{4}{3}\,\sigma_\mathrm{T} \left(\frac{P_\mathrm{e}}{m_\mathrm{e}\, c}\right)^2 \left(\frac{B_\mathrm{o}^2}{8\,\pi}\,\mathrm{H}(P_\mathrm{e}-\tilde{P}_\mathrm{e}) + U_\mathrm{ph}\right) \tag{18}$$

the cooling function. U_ph is the photon energy density, which is dominated by the MWB, and H is the Heaviside step function, used as an approximation of the sharp change in opacity. The height of the step is therefore

$$\lim_{\delta\to 0} \frac{N_\mathrm{e}(\tilde{P}_\mathrm{e}-\delta)}{N_\mathrm{e}(\tilde{P}_\mathrm{e}+\delta)} = \frac{B_\mathrm{o}^2}{8\pi\, U_\mathrm{ph}} + 1 \tag{19}$$

The exact shape of the transition is a little bit more complicated to calculate, since the problem is nonlinear due to the mutual dependence of the electron spectrum and the absorption coefficient, the geometry of the radiation transport, which has to be considered, and the time dependence before establishing the

equilibrium spectrum. For a field of e.g. $B_o = 10\,\mu$G a step in the electron spectrum of one order of magnitude is expected at $P_e = 26$ MeV/c (using our simple approach), very close to the position of the expected flattening below the injection peak in the *secondary electron model*. The *in-situ acceleration model* predicts no step at this energy, since the cooling function determines only the high energy cutoff region of the spectrum, where the cooling gets comparable to the acceleration. We note, that any break in the electron spectrum below the observed range would lower the effect of synchrotron self absorption. Assuming a break in the radio spectrum at 30.9 MHz as in Sect. 3.2 shifts the step in the above example to 15 MeV/c.

5. Conclusion

The search for diffuse emission in any photon energy band leads to interesting information about the shape of the relativistic electron population in the Coma cluster of galaxies. We present a compilation of several limits, and discuss spectral features of the electrons within the various radio halo formation models. A signature in the low energy range is expected to arise from the sharp change in opacity for low frequency radio photons due to synchrotron self absorption, which could distinguish between a relativistic electron population which is cooling and one which is gaining energy, as it is predicted for *primary* and *secondary electron models* on the one hand, and for *in-situ acceleration models* on the other hand. Another signature of the *secondary electron model* is a flattening of the spectrum below the main electron injection energy. Future observations of diffuse emission might test the electron distribution sensitively enough in order to see these signatures. Present observations restrict the electron population sufficiently, so that a central magnetic field strength higher than $1.2\,\mu$G is needed in order to explain the observed synchrotron emission, if the steep volume integrated radio spectrum with spectral index of 1.34 can be extrapolated to lower frequencies, or a limit of $B_o > 0.3\,\mu$G, if a break appears below the observed range. Since these limits arise from a detected EUV flux excess, which is interpreted to result from a cool gas component of the intra cluster medium, the possibility remains, that this flux results in fact from inverse Compton scattering of microwave photons, if the field strength is below $1.2\,\mu$G. This possibility seems to be in contradiction with the Faraday measurement of Feretti et al. (1995) of $6\,\mu$G. But since the inverse Compton argumentation gives volume averaged field strength which are weighted with the relativistic electron distribution, stronger field strength in regions with a low density of relativistic electron could solve this contradiction. If the nature of this EUV excess can be understood theoretically, the EUV limit on inverse Compton flux might be improved and a higher field strength limits might result.

Limits without extrapolation of the electron spectrum come from the scattering of starlight photons to EGRET energies ($B_o > 0.1\,\mu$G) and microwave photons to OSSE energies ($B_o > 0.2\,\mu$G). Magnetic field limits from inverse Compton limits are below the estimates resulting from Faraday rotation measurements, being therefore in good agreement. They measure the magnetic content of the Coma cluster on a more global scale, and demonstrate independently that the observed Faraday rotation results from magnetic fields within the intra cluster medium. Future EUV, X- and gamma-ray telescopes will raise these limits on the magnetic field strength in the Coma halo region to the level of Faraday measurements, or they will detect energetic nonthermal photons from Coma, resulting from inverse Compton scattering or from other sources.

Acknowledgements. T.A.E. is supported by the *Studienstiftung d. dt. Volkes*. We acknowledge discussions with Richard Lieu and useful comments by Jack O. Burns.

Appendix A: Transrelativistic Thomson scattering

We follow the derivation of the formulae of transrelativistic Thomson scattering by Wright (1979). Scattering of a photon from an isotropic photon field by an electron with velocity $\beta_e\, c$ and energy $\gamma_e\, m_e\, c^2$ has a probability distribution of the angle θ between photon and electron direction in the electron's rest frame given by

$$f(\mu)\, d\mu = [2\gamma_e^4(1-\beta_e\mu)^3]^{-1}\, d\mu\ , \tag{A1}$$

where $\mu = \cos\theta$. The logarithmic frequency shift from ν to ν' of the photon after scattering into an angle θ' is

$$s = \ln\left(\frac{\nu'}{\nu}\right) = \ln\left(\frac{1+\beta_e\mu'}{1-\beta_e\mu}\right)\ . \tag{A2}$$

The probability distribution of $\mu' = \cos\theta'$ for a given μ is

$$g(\mu';\mu)\, d\mu' = \frac{3}{8}[1+\mu^2\mu'^2 + \frac{1}{2}(1-\mu^2)(1-\mu'^2)]\, d\mu'\ . \tag{A3}$$

The probability for a shift s given the electron velocity is

$$P(s;\beta_e)\, ds = \left[\int d\mu\, f(\mu)\, g(\mu';\mu)\, \left(\frac{\partial\mu'}{\partial s}\right)\right]\, ds\ . \tag{A4}$$

$\mu'(s,\beta_e,\mu)$ is given by (A2) and the range of integration is given by the conditions $-1 < \mu < 1$ and $-1 < \mu' < 1$. Rephaeli (1995) simplified this integral by assuming that the scattering is isotropic in the electron's rest frame, which allows to average over the angle between background and scattered photon. He compared scattered photon spectra using the simplified and exact formulae numerically, and found no significant difference for electrons with energies of 1...15 keV, typical for the thermal component of the ICM. But suprathermal electrons, expected to be the connection between the thermal and the halo electrons, see an anisotropic photon field in their rest frame. Fortunately, the integrand in (A4) is a rational function of μ and therefore analytically integrable. Integrating the two regimes $s < 0$ and $s > 0$ separately and introducing the dimensionless momentum $p = \beta_e\,\gamma_e$ leads to:

$$P(s,p) \;=\; \frac{3e^s(1+e^s)}{8p^5}\left[\frac{3+3p^2+p^4}{\sqrt{1+p^2}} - \frac{3+2p^2}{2p}(\tilde{s}-|s|)\right]$$

$$+\frac{3\mathrm{sgn}(s)}{32p^6}\left[1-e^{3s}+3e^s(1-e^s)(9+8p^2+4p^4)\right] \qquad \text{(A5)}$$

The maximal logarithmic frequency shift is given by

$$\tilde{s} = \ln\left(\frac{1+\beta_\mathrm{e}}{1-\beta_\mathrm{e}}\right) = \ln\left(\frac{\sqrt{1+p^2}+p}{\sqrt{1+p^2}-p}\right) \ , \qquad \text{(A6)}$$

and therefore is $P(s,p) = 0$ for $|s| > \tilde{s}$. The distribution of frequency shifts of scattering with a spectrum of electrons $n_\mathrm{e}(p)\,dp$

$$P(s)\,ds = \frac{\int\, dp\, n_\mathrm{e}(p)\, P(s;p)}{\int\, dp\, n_\mathrm{e}(p)}\, ds \qquad \text{(A7)}$$

has to be folded with the photon spectrum $n(\nu)\,d\nu$ in order to obtain the source spectrum of scattered photons

$$q(\nu')\,d\nu' = \sigma_\mathrm{T}\, c\, n_\mathrm{e}\, \left[\int_{-\infty}^{+\infty} ds\, P(s)\, n(\nu'\, e^{-s})\right] d\nu' \ . \qquad \text{(A8)}$$

These formulae can be applied from non- to ultrarelativistic electron momentum, they are valid for scattering to higher and lower energies compared with the background photon energy, but they are restricted to the Thomson regime ($h\,\nu \ll \gamma_\mathrm{e}\, m_\mathrm{e}\, c^2$). Applications are especially IC scattering by transrelativistic electrons, such as suprathermal electrons, or electrons of a very hot plasma. Since the evaluation of (A5) needs only a little more computation time than its approximations, it could be included in any numerical code for Thomson scattering.

References

Abramowitz M., Stegun I.A., 1965, Handbook of Mathematical Functions. Dover, New York

Blumenthal G.R., Gould R.J., 1970, Rev. Mod. Phys. 42, 237

Briel U.G., Henry J.P., Böhringer H., 1992, A&A 259, L31

Burns J.O., Roettiger K., Ledlow M., Klypin A., 1994, ApJ 427, L87

Deiss B.M., Reich W., Lesch, H., Wielebinski R., 1997, A&A 321, 55

Dennison B., 1980, ApJ 239, L93

Dixon W.V., Hurwitz M., Ferguson H.C., 1996, ApJ 469, L77

Enßlin T.A., Biermann P.L., Kronberg P.P., Wu X.-P., 1997, ApJ 477, 560

Feretti L., Dallacasa D., Giovannini G., Tagliani A., 1995, A&A 302, 680

Girardi et al., 1995, ApJ 438, 527

Henning P., 1989, AJ 97, 1561

Jaffe W.J., 1977, ApJ 212, 1

Kim K.-T., Kronberg P.P., Dewdney P.E., Landecker T.L., 1986, In. O'Dea C.P. & Uson J.M. (eds.) NRAO Proc., Radio Continuum Processes in Clusters of Galaxies. Green Bank, p. 199

Kim K.-T., Kronberg P.P., Dewdney P.E., Landecker T.L., 1990, ApJ 355, 29

Lieu R. et al., 1996, Science 274, 1335

Novikov I.D., Thorne K.S., 1972, In. DeWitt C. & DeWitt B.S. (eds.), Black Holes. Les Houches, Gordon and Breach, New York, p. 342

Schlickeiser R., Sievers A., Thiemann H., 1987, A&A 182, 21

Secker J., Harris W.E., 1996, ApJ 496, 623

Sreekumar et al., 1996, ApJ 464, 628

Strom K.M., Strom S.E., 1978, AJ 83, 73

Rephaeli Y., Ulmer M., Gruber D., 1994, ApJ 429, 554

Rephaeli Y., 1995, ApJ 445, 33

Roland J., 1981, A&A 93, 407

Rybicki G.B., Lightman A.L., 1979, Radiative Processes in Astrophysics. Wiley, New York

Wise M.W., O'Conell R.W., Bregman J.N., Roberts M.S., 1993, ApJ 405, 94

Völk H.J., Aharonian F.A., Breitschwerdt D., 1996, Space Sci. Rev. 75, 279

Waldthausen, H., 1980, Ph.D.Thesis, University of Bonn, Germany

Wright E.L., 1979, ApJ 232, 348

Webbink R.F., Jeffers W.Q., 1969, Space Sci. Rev. 10, 191

This article was processed by the author using Springer-Verlag LaTeX A&A style file *L-AA* version 3.